POWER CONVERTER FOR DC BUS SHARING TO INCREASE THE ENERGY EFFICIENCY IN DRIVE SYSTEMS

Davis Meike

Daimler AG
Robotics and Technology Units
(PKL/AST), Germany
davis.meike@daimler.com

Armands Senfelds, Leonids Ribickis

Riga Technical University
Institute of Industrial Electronics and
Electrical Engineering (IEEI), Latvia
armands.senfelds@rtu.lv, leonids.ribickis@rtu.lv

ABSTRACT

It is state of the art for many drive systems like those used in industrial robotics, conveyor systems or diverse numerical control machinery to have a common DC bus power system architecture. Due to regenerative braking, the DC bus voltage increases until a certain limit, which is limited means of a balancing resistor (brake chopper). Systems that require rapid cyclic starts and stops are subject to significant energy waste due to extensive use of the brake chopper.

In this article, a novel power converter for drive systems is proposed that allows the brake chopper to be omitted and enables the exchange of regenerative energy among multiple drive systems within an independent DC subgrid with one centralized energy storage element. The solution does not require identical hardware or exact synchronization between the drive rectifiers, therefore it is applicable to both existing and new production equipment alike. Experimental results in industrial robot drives show savings of up to 20%.

1. INTRODUCTION

Due to complex production requirements, many industrial production applications often require rapid motion control - fast accelerations and reversals are usual. In particular, industrial robots that are typically equipped with several actuators connected in one kinematic chain have a high peak power requirement compared to their average power. It is state of the art for multiple motor drives in one system to be supplied by a single DC power source - an AC rectifier. Despite the fact that existing drive systems today are normally capable of regenerative braking, the recuperated energy is rarely fed back to a network or stored locally due to AC network quality conservation issues or increased costs of the storage systems.

Common DC link applications using a single rectifier and multiple variable frequency drives have been state of the art for many years. Multiple rectifiers and multiple drives that *share* the DC links are typical in some high-power variable frequency drives with nominal power ratings reaching several megawatts in order to equalize the load between IGBT switches. Modular DC bus sharing for functional purposes in a lower power range is available from some manufacturers [1]. Some examples are known from wind power turbines [2] and active power filters [3]. Actual research trends in future power system development present applications of DC transmission and distribution technologies as well like presented in [4]. Commercially available DC distribution system solution for maritime propulsion drives and discussion on potential optimizatoin has been presented [5]. DC based distribution as aircraft application has been discussed [6] as well as comparison on various poweer conversion stages regarding power density of converters. Therefore future integration of industrial production applications based on DC distribution are matter of interest. Analytical research of shared/common DC bus operation can also be found in [7].

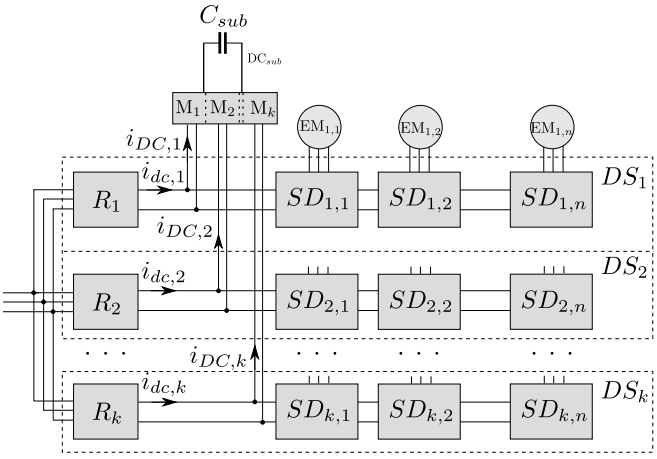

Fig. 1. A shared DC bus configuration with power converters

ISBN 978-1-4799-0224-8

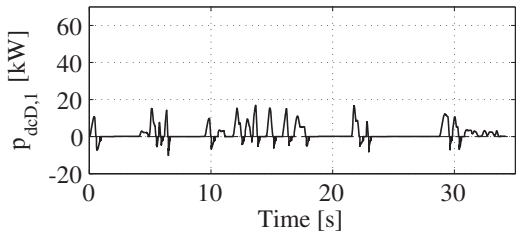

Fig. 2. Consumption of a single robot, $k = 1$

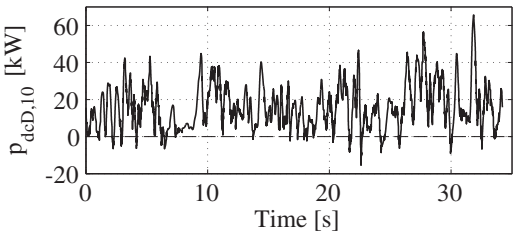

Fig. 3. Consumption of shared robot DC buses, $k = 10$

However, in all these cases, synchronized control of the drive switches is required so that these DC links are equalized. In fact, there is actually one synchronized DC bus that is supplied by more than one parallel rectifier. The previous research by the authors includes an alternative solution for drive sharing in [8] that does not require drive-to-drive synchronization. Using a common-ground power converter, the authors show how any drive system can store its recuperative excess energy in an independent DC subgrid, which can supply the power back when needed. Despite the fact that the solution showed significant energy savings, a common negative-pole connection caused the circular currents between drive systems. In this paper, a power converter uses semiconductor switches in both positive and negative poles of the DC bus to eliminate the side effects. A use case in robotic production with a shared/common DC bus is proposed in [9].

Fig.1 depicts an architecture where DC buses of drive systems are not connected in parallel directly. Instead, power converters are used as the interface between drive systems. Here, k drive systems $DS_1, \ldots, DS_k$ are used where each supplies n servo drives $SD_{i,1}, \ldots, SD_{i,k}$. A servo drive $SD_{i,j}$ supplies an electrical machine $EM_{i,j}$. Each of the DC buses $DC_1, \ldots, DC_k$ are connected to the power converter modules $M_1, \ldots, M_k$. Each module is connected to a subgrid DC_{sub}, so that any module M_i is parallel to any other M_{i+1}. The capacitor C_{sub} determines the size of the energy exchange buffer.

In the following, the Section 2 discusses high-level simulation of power consumption in robotic production. Section 3 describes the proposed power converter unit. Section 4 presents the modeling results of power electronics, but Section 5 provides the experimental validation and viability proof of implementation for industrial robots.

2. HIGH-LEVEL SIMULATION OF INDUSTRIAL ROBOT CONSUMPTION

The simulation was conducted as a reference program using high-payload robot system model as in [10]; the power consumption profiles were compared virtually. A power requirement for the industrial robots connected with shared DC buses is calculated in the form

$$p_{dcD,k}(t) = \sum_{i=1}^{k} (p_{dc,i}(t) - p_{D,i}(t)) \tag{1}$$

where p_{dc} is the power consumption within a DC bus, p_D is the power loss on the brake chopper, and k denotes the number of shared robots. The negative part of the power curve is

$$p^*_{[dcD],k}(t) = \begin{cases} -p_{[dcD],k}(t) & \text{if} \quad p_{[dcD],k}(t) \leq 0, \\ 0 & \text{if} \quad p_{[dcD],k}(t) > 0. \end{cases} \tag{2}$$

The start of the sample robot program has randomly been shifted within in the range $[0 \ldots \frac{\text{duration}}{2}]$. Fig.2 and Fig.3 show the respective power curves for $k = 1$ and $k = 10$. It can be seen that there are fewer negative power peaks than in the case of a single robot. The positive power peaks of the single robot power exceed 17 kW, whereas the maximum peak in the case of ten robots sharing the DC bus is below 65 kW.

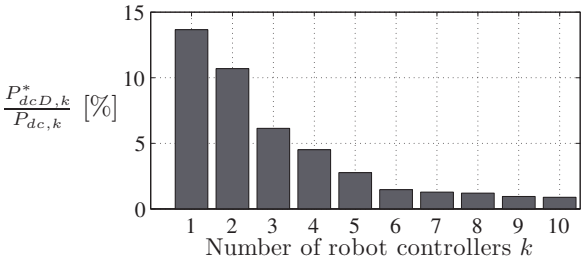

Fig. 4. Energy proportion dissipated on balancing resistors as function of k

The modeling results of varying numbers of shared robot drive systems are shown in Fig.4, where $P^*_{dcD,k}$ is the average dissipated power for k drive systems, but $P_{dc,k}$ is average total consumption of k drive systems. For a single robot, the dissipated average power is $P_D = 276W$, which corresponds to 14.8% of the power requirement within a DC bus (no static losses of the control cabinet considered here). The average dissipated power drops with each additional robot drive system added to

the DC subgrid. With five robots, the dissipated energy of all robot drives is below 3.2% (264 W), but with ten robots it is as low as 1.1% (175 W) of the energy requirement on the DC bus of the respective amount of robots involved..

3. POWER CONVERTER MODULE

In order to enable the flow of electrical power in a controlled manner, an electrical circuit as represented in Fig.5 is proposed. The general structure, the main circuit elements and the application of the subgrid interface module applied are explained in section 4.2. Power flow control considering specific application constraints and the applied technique are discussed in section 3.2. Detailed operation of the proposed circuit is discussed in section 3.3.

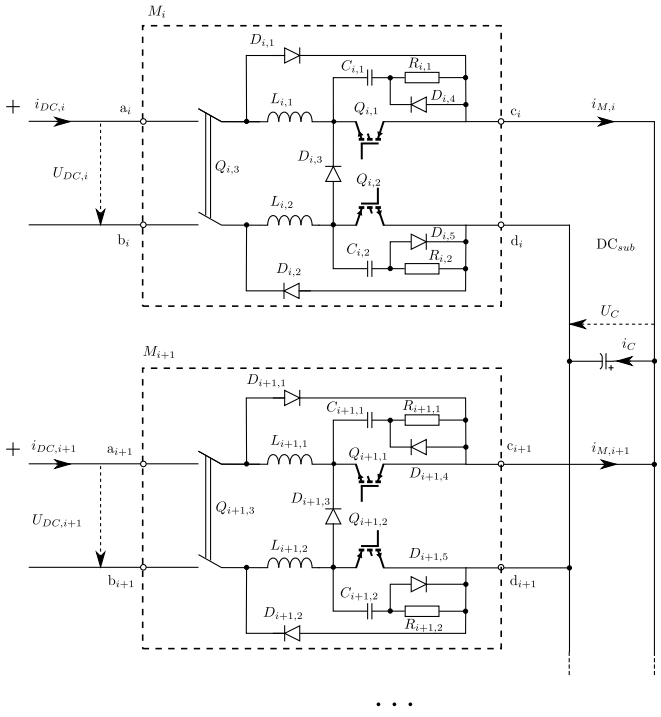

Fig. 5. Electrical circuit of DC subgrid interface module

3.1. Proposed electrical circuit

The electrical circuit enables a bidirectional power flow between individual drive systems DS_i, DS_{i+1} and subgrid DC_{sub}. The module M_i has 4 terminals a_i, b_i, c_i and d_i, where terminals a_i and b_i are connected to the positive and negative poles of a particular DC bus DC_ii and terminals c_ii and d_i are connected to terminals c_{i+1} and d_{i+1} of the other module respectively. A central capacitor C_{sub} is connected between all terminals $c_{1\ldots k}$ and $d_{1\ldots k}$. The applied circuit allows symmetric disconnection of positive and negative DC connection terminals by means of simultaneous commutation of IGBT semiconductor switches $Q_{i,1}$ and $Q_{i,2}$ avoiding common ground operation as discussed in [8]. Mechanical disconnection of poles for safety reasons is realized by means of contactor $Q_{i,3}$. Inductors $L_{i,1}$ and $L_{i,2}$ are utilized for current damping during coupling of the storage capacitor and drive DC bus.

3.2. Power flow control principles

Since the objective of the proposed system is the storage and utilization of excess electrical energy being generated during recuperation, the system should not influence normal operation when power is taken only from the AC grid. The presence of the recuperation process can be observed since unidirectional rectifiers are applied and energy is stored in smoothing capacitors resulting in a rise of the individual drive DC bus voltages $U_{DC,i}$. The DC bus voltage level corresponding to normal operation from the AC grid can be calculated as

$$U_{dc,idle} = \sqrt{2}U_{rms} \approx 565V. \tag{3}$$

Therefore, a hysteresis type control of storage capacitor voltage U_C is applied in order to utilize excess energy and prevent the discharge of the storage capacitor below (3) to disable direct recharging from the AC grid by rectifier instead of recuperation according to (4), where S_{t+1} represents IGBT switch states of the next simulation time step.

$$S_{t+1} = \begin{cases} 0 & \text{if } U_C \leq U_{off} \text{ and } U_C \leq U_{on}. \\ 1 & \text{if } U_C > U_{off} \text{ and } U_C > U_{on}. \\ S_t & \text{otherwise,} \end{cases} \tag{4}$$

In order to reduce high current peaks arising from the coupling of the storage capacitor and each drive system's DC bus, the voltage difference U_Δ has to be taken into account:

$$U_\Delta = U_C - U_{DC,i}. \tag{5}$$

3.3. Operating modes

During normal operation of the DC subgrid module, contactor $Q_{i,3}$ remains closed and is disconnected in the eventof an unexpected state for safety reasons or maintenance purposes. The charging of the main energy storage unit in DC_{sub} is enabled by natural commutation of diodes $D_{i,1}$ and $D_{i,2}$ when, as a result of the recuperation of DS_i, its voltage $U_{DC,i}$ has increased above the actual subgrid voltage U_C enabling the charging process that results in a positive current $i_{DC,i}$.

The discharging of the subgrid is enabled in a controlled manner through the control of IGBT switches

$Q_{i,1}$ and $Q_{i,2}$. The negative current flow is determined by voltage difference U_Δ according to (5) and inductors $L_{i,1}$ and $L_{i,2}$. When a storage capacitor with the respective voltage U_C has reached a voltage level U_{off} applied for control as in (4), the current $i_{DC,i}$ is interrupted. Since magnetic energy has been stored in $L_{i,1}$ and $L_{i,2}$ during discharge operation, the current freewheeling path is realized by diode $D_{i,3}$ in order to avoid high voltage during turn-off of IGBT elements. The RCD snubber circuit for reduction of overvoltage stress of the IGBT switches has been implemented by combination of elements $R_{i,1}$, $C_{i,1}$ and $D_{i,4}$ regarding snubber of IGBT $Q_{i,1}$ in this particular case as an example. Diodes $D_{i,7}$ and $D_{i,8}$ ensure that no reverse conduction via an alternative charging current path is possible in the case when IGBT switches are enabled.

4. FUNCTIONAL SIMULATION

In order to examine the feasibility of the proposed system, numerical simulation has been applied based on a model of the electrical system implemented by means of a Matlab simulation model. The design approach of the numerical model has been described in section 4.1. The character and origin of the chosen electrical load simulation input data and the results obtained by numerical simulation are evaluated in section 4.2.

4.1. Structure of applied simulation model

The proposed electrical circuit simulation model has been developed according to the functional layout presented in Fig.1; however, reduced to a system with $k = 2$ interconnected drive systems via a shared DC bus. The size of the energy exchange buffer unit C_{sub} has been selected to be 45 mF, representing a real capacitor bank available for the field experiment stage of development. The respective power converter modules M_1, M_2 have been developed according to the electrical circuit depicted in Fig.5. A common power grid of 50 Hz frequency is assumed and implemented as an AC voltage source. Typical brake chopper functionality is modeled: a resistor is triggered if $U_{DC,i} \geq 680V$.

4.2. Simulation results

The performance of the proposed electrical system can be analyzed by examination of electrical quantity time variation. Two industrial robot load profiles were selected as input data. The chosen profiles present a peak load of $18kW$ as well as recuperation with a maximum of $10kW$ generated power within an operation period of 11 seconds. Applied power profile has been obtained by single robot power consumption of industrial robot during handling operation. Over the operation period, both robots result in average power of $7.49kW$.

The expected operation of a control algorithm and the estimated electrical system behavior resulting in $U_{DC,i}$ variation and the respective current flow regarding commutation of the power semiconductors can be observed in Fig.6. The chart at the top of the figure represents the actual power being consumed or generated by each of two drive systems, namely DS_1 and DS_2. The DC bus voltage variation of $U_{DC,1}$, $U_{DC,2}$ and the interconnected U_C part is shown in the second chart down. The third chart down represents the actual current flow from DS_1 and DS_2 to a subgrid as $I_{DC,1}$ and $I_{DC,2}$ as well as a current flow to the storage capacitor I_c. The bottom chart displays the switching states of $Q_{i,1}$ and $Q_{i,2}$ of M_1 and $M2$ respectively. The following processes can be examined:

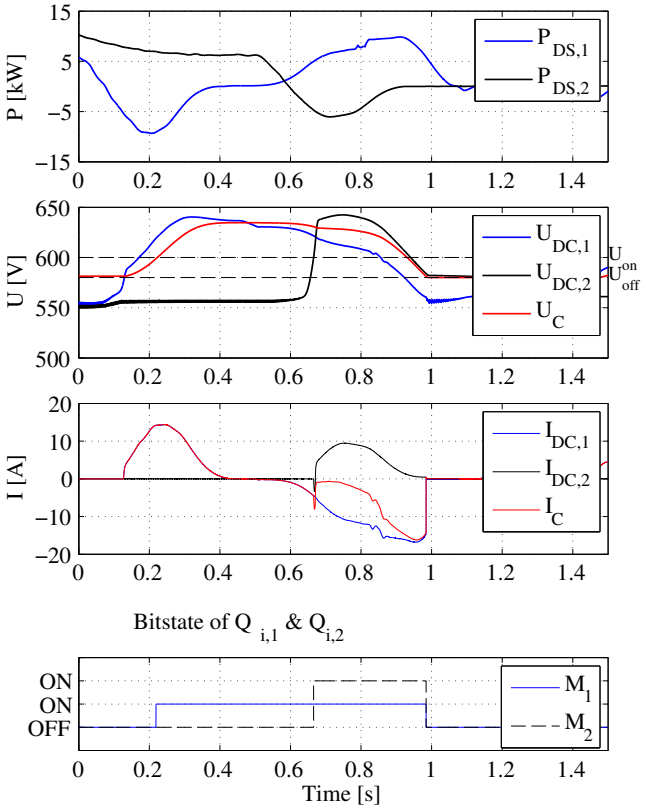

Fig. 6. Simulation of energy exchange between drive systems and asynchronous switching at voltage control levels: 580 V and U_{on} 600 V, allowed voltage difference for coupling U_Δ ≤20V.

- $t = 0 : 21s : DS_1$ has raised the DC subgrid voltage using the recuperation process, the discharge of energy storage of DS_1 is enabled. DS_2 needs power requirement and a discharge of stored energy is not allowed since the voltage difference U_Δ is too large.

- $t = 0 : 65s$: The recuperation process and the voltage increase of DS_2 enable coupling with a shared DC bus. The energy flow from DS_2 to DS_1 via the shared DC bus with a storage capacitor is started.
- $t = 1s$: The shared DC bus voltage U_C reaches a threshold U_{off} and further discharge of the energy storage unit is disabled.

The influence of a control voltage variation on system performance has been observed by a sequence of simulations. The lower control voltage U_{off} has been varied in a range from 560 V to 670 V. A turn-on voltage level U_{on} has been applied 20 V higher than U_{off}.

The reduction in average power achieved per cycle versus the variation of the control threshold is presented in Fig.7. It is obvious that a larger portion of saved energy is present at lower turn off threshold voltage U_{off}; this is a result of better utilization of the energy storage unit leading to a longer discharge process.

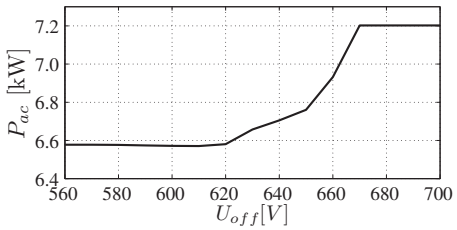

Fig. 7. P_{ac} as a function of U_{off}

5. EXPERIMENTAL VALIDATION

For circuitry and functionality experimental validation, two industrial robots have been selected being utilized in typical production facility: Quantec series with a payload of 210 kg and a KRC4 controller. Both drive systems are connected with modules according to Fig.5. Further configuration parameters include tool load masses 154 kg and 210 kg, the robot application represents sample handling operations programmed with 75% execution velocity. Fig.8 shows the general example of the recuperative energy exchange between both drive systems and a DC subgrid.

General functionality. The measured functionality is shown in Fig.8.The C_{sub} charging is present when the sum of $I_{DC,1}$ and $I_{DC,2}$ is positive. Various processes can be recognized during operation:

- $t = 0.5s$: Recuperation of DS_1.
- $t = 0.6s$: Recuperation of DS_2.
- $t = 1.8s$: Recuperation of DS_2, which causes the U_C increase above U_{on} that triggers to switch-on $Q_{2,1}$ and $Q_{2,2}$ of the module M_2.
- $t = 2.3s$: Supply of DS_2.
- $t = 2.5s$: Recuperation of DS_1, during which $U_{DC,1}$ independently increases above $U_C - U_k$. Here, a direct energy exchange can be observed - DS_2 is supplied from M_1 and C_{sub}.
- $t = 2.8s$: Recuperation of DS_1 is over. DS_1 is supplied by C_{sub} only until U_C falls below U_{off}, when IGBT switches $Q_{i,1}$ and $Q_{i,2}$ of both modules M_1 and M_2 are switched off.
- $t = 3.7s$: recuperation of DS_2 - the process repeats as in the first step.

Therefore, the measurement results comply with the expected control algorithm. A voltage sensor delay may be observed - the $Q_{i,1}$ and $Q_{i,2}$ switching, in fact, is initiated when U_C is well below U_{off}.

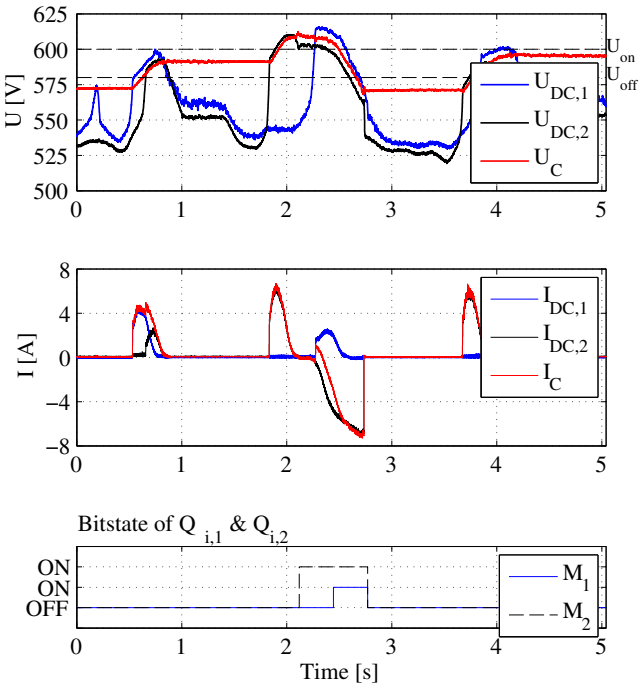

Fig. 8. Measurement of the energy exchange between robot drive systems; $U_{on} = 580V$, $U_{off} = 600V$

Energy consumption measurements. The power requirement on the AC supply side of both coupled industrial robots has been measured over operation period. The results show the energy consumption reduction up to 22.7% in a coupled DC bus configuration over a state-of-the-art systems. Since robot energy consumption is strongly dependent on its tool load, velocity, motor temperature and other parameters, several measurements have been conducted in a sequence, from which some are summarized in Table 1. The average power consumption is significantly higher with a higher tool load; however, the energy savings proportion remain approximately similar. Since only cyclic handling process alike movements

Table 1. Energy consumption measurement results with three-semiconductor switch power modules

Application type	Duration [min]	Velocity [%]	Tool [kg]		Temp. [K]		DC-bus sharing	Avg. power [kW]	Difference [%]
			R1	R2	R1	R2			
Handling	20	100	0	0	333	333	none	6.23	-
Handling	20	100	0	0	331	331	√	4.92	-21.1%
Handling	20	100	154	204	341	341	none	8.67	-
Handling	20	100	154	204	347	347	√	6.70	-22.7%

have been measured, the production standstills in manufacturing process must be considered when estimating the average savings on an annual scale.

6. CONCLUSIONS

This paper presents a new type of power converter for DC bus sharing to increase the energy efficiency of production machines utilizing electrical drives with recuperation possibility. Regenerative energy in machine tools may vary from 10% to 25% of total consumption depending on the application. However, due to expensive energy storage elements or bidirectional rectifiers at AC supply side, it is rarely reused effectively and dissipated at the DC bus braking resistor (i.e. brake chopper).

Simulation results show that the total volume of single, shared electrical energy storage units can be dimensioned much smaller than the sum of multiple separate storages, one each per production machine. The modular power interface system is proposed to enable the exchange and storage of the regenerative braking energy. The functionality of a power module is both simulated and experimentally validated.

The proposed power converter system is applicable to any state-of-the-art drive system with a rectifier, common DC bus and one or more inverters, such as those used in robotics, conveyors and diverse machine tools. The viability is proved using two high-payload industrial robots (KUKA Quantec series KR210 with KRC4 controllers) showing energy savings of over 20%. For implementation, the drive systems do not require any internal synchronization, nor identical components or hardware modifications to be attached to a shared DC subgrid with an energy storage element. Instead, the originial equipment may eventually even be downsized by eliminating or reducing number of utilized the DC bus brake chopper units.

7. REFERENCES

[1] Allen-Bradley, *PowerFlex AC Drives in Common Bus Configurations*, Rockwell Automation, 2011.

[2] Li Meng and Wang Yong, "Research on the parallel technique for the direct-drive wind power converter," in *Electrical Machines and Systems (ICEMS), 2011 International Conference on*, Aug. 2011, pp. 1 – 4.

[3] Prasad N. Enjeti Lucian Asiminoaei, Eddy Aeloiza and Frede Blaabjerg, "Shunt active-power-filter topology based on parallel interleaved inverters," in *IEEE Transactions On Industrial Electronics*, 2008.

[4] Florian Mura and Rik W. De Doncker, "Preparation of a medium-voltage dc grid demonstration project," Tech. Rep., E.ON Energy Research Center, 2011.

[5] T.Myklebust J.F. Hansen, J.O. Lindtjorn and K. Vanska, "Onboard dc grid, the newest design for marine power and propulsion systems," Tech. Rep., ABB Corp., 2013.

[6] A. Lucken D. Schulz J. Brombach, T. Schroter, "Optimized cabin power supply with a +/− 270 v dc grid on a modern aircraft," in *Compatibility and Power Electronics (CPE), 2011 7th International Conference-Workshop*, 2011.

[7] A.H. Wijenayake, T. Gilmore, R. Lukaszewski, D. Anderson, and G. Waltersdorf, "Modeling and analysis of shared/common dc bus operation of ac drives.," in *Industry Applications Conference, 1997. Thirty-Second IAS Annual Meeting, IAS '97., Conference Record of the 1997 IEEE*, Oct. 1997, vol. 1, pp. 599 – 604.

[8] D. Meike and I. Rankis, "New type of power converter for common-ground dc bus sharing to increase the energy efficiency in drive systems," in *Energy Conference and Exhibition (ENERGYCON), 2012 IEEE International*, 2012, pp. 225–230.

[9] Michael Lebrecht and Thomas Schneider, "Robotersystem," patent P817837, Deutsches Patent- und Markenamt, 2010.

[10] Davis Meike, "Multi-domain model for the evaluation of large scale robotic applications within production," in *Proceeding of the 53nd Annual International Scientific Conference of Riga Technical University*, 2012.